A novel metal-organic frameworks based humidity pump for indoor moisture control

Pumin Hou, Kan Zu, Menghao Qin*, Shuqing Cui

Department of Civil Engineering, Technical University of Denmark, Lyngby, 2800, Denmark

*Corresponding author: E-mail address: menqin@byg.dtu.dk

Abstract

Latent heat load accounts for a significant proportion of energy consumption by air-conditioning, particularly for buildings in humid climates. Traditional vapor-compression refrigeration dehumidification faces problems like refrigerant leakage, overcooling, and complicated mechanical systems. Here, we report a novel humidity pump that uses metal-organic frameworks (MOFs) as desiccant layers to transport moisture from a low-humidity space to a high-humidity one efficiently. The working principle and operation modes of the humidity pump are introduced herein for which the dehumidification performance is investigated at 22.8 ◦C with 60% RH. The dehumidification rate and moisture removal efficiency of the MIL-100(Fe) based humidity pump reached 26.24 g h^{-1} and 0.87 g Wh^{-1}, respectively, and these are 2.15 and 2.12 times higher than that of the humidity pump with silica gel coating. The maximum dehumidification coefficient of performance (DCOP) of the humidity pump could reach up to ~0.46, higher than the conventional desiccant dehumidification systems. In addition, many factors, such as the cycle time, thermoelectric power, air velocity, etc., which may affect the dynamic characteristics and dehumidification

performance, were analyzed. Lastly, the localized humidity management ability of the designed humidity pump using MIL-100(Fe) was validated by a small chamber test. The results indicate that the MOF humidity pump could achieve energy-efficient localized moisture control.

Keywords: Metal-organic frameworks; Humidity pump; Dehumidification performance; Localized moisture control.

1. Introduction

Energy consumption by buildings has become a worldwide concern. The building sector consumes 40% of the global energy, which is mainly provided by fossil fuels and corresponds to over one-third of carbon dioxide emissions [1,2]. The air conditioning systems account for a significant proportion of the total energy requirement in our living environments.

It is worth noting that the latent heat load makes a large proportion of energy for air handling and particularly for buildings in humid climates [3]. Overall, the latent heat load takes up to 20–40% in the air conditioning system [4]. Vapor-compression refrigeration system based on cooling dehumidification is commonly used for indoor temperature and humidity control. During the dehumidification process, the temperature of the air is reduced to the point that is below the dew point in order to condense it. However, this dehumidification method makes the air temperature too low to be directed to the room and needs to be reheated, which causes wastage of energy [5]. By raising the evaporation temperature of 1 ◦C, the COP of a vapor compression refrigeration system can be increased by about 2.8%, and thus the energy

consumption can be decreased by about 2.5% [6,7]. If the treatment of the latent heat load can be decoupled from the sensible cooling, reducing the temperature of the evaporator to such a low level will not be required. Moreover, it is difficult for vapor compression systems to operate with high performance in small space humidity control applications due to their bulk and complex systems [8]. Therefore, there is a necessity to develop a novel moisture control device for localized humidity management with high efficiency.

To remove the latent heat load separately, many efforts have been dedicated to technologies such as solid dehumidification [9,10], liquid desiccant dehumidification [11,12], membrane dehumidification [13, 14], etc. Combining these dehumidification methods with low-grade energy sources like solar energy and heat pumps can improve dehumidification and energy efficiency [15–17]. However, shortcomings and limitations of these dehumidification methods, such as the problem of re-cooling in rotary solid dehumidification, the growth of bacteria in liquid desiccant dehumidification, have not been solved.

In order to avoid the fresh air dehumidification and to improve air conditioning efficiency, several studies have been done about coating desiccant on the surface of evaporators and condensers [18,19]. Chai et al. combined a desiccant coated heat exchanger (DCHE) with a heat pump for energy saving [20]. Andres et al. investigated the performance of silica gel and sodium acetate composite coated heat exchanger in the summer and winter season [21]. In this case, however, the solid desiccant used is silica gel and its high regeneration temperature reduces the performance of the device significantly. Cui et al. chose porous metal-organic frameworks (MOFs) as advanced sorbents instead of the traditional solid desiccant for which the COP of 7.9 was achieved, demonstrating the superiority of this material [22].

The concept of a humidity pump is inspired by a heat pump. A humidity pump is a device that can transport moisture through the inverse gradient of vapor concentration, i.e., the vapor can be transferred from a relatively low-humidity space to a high-humidity space. For example, in summers, the humidity pump will transfer moisture from cool and less humid indoor condition to a hot and humid outdoor condition; vice versa, in winters. Li et al. [8] designed a full-solid-state humidity pump based on silica gel, which exhibited good humidity transfer performance without using refrigerant or cooling water. However, the device is limited to the efficiency of mass transfer, and the motor to achieve continuous operation increases the complexity of the device.

Desiccants play an important role in the humidity pump. Traditional desiccants such as silica gel and zeolites possess low adsorption capacity and poor regeneration ability and this limits the development of the adsorption dehumidification system. Though a composite desiccant (silica gel-based, carbon-based, etc.) has been prepared by impregnating hygroscopic salt to enhance the adsorption capacity [23], hygroscopic salts are unstable and deliquesce easily under high humidity.

Metal-organic framework (MOF) is a new type of porous crystalline material formed by self-assembly of inorganic metal ions and organic ligands. MOFs possess many good properties like huge internal surface area, large micropore volume, physicochemical and chemical variability as well as low regeneration temperature [24,25]. Although traditional inorganic porous desiccant has been investigated for a humidity pump, the application of MOFs in humidity pump is still worth investigating owing to its high potential in moisture transfer.

In the present study, a humidity pump based on MOFs is fabricated, and its working principle

and operation mode are introduced. The performance and impact factors of the device have also been investigated by experiments under different conditions. The localized moisture control ability of the device has been tested experimentally, which provides an important insight to precise moisture control in a confined space.

2. Methodology

2.1 Humidity properties of MIL-100(Fe)

Methyl methacrylate (MMA), n-octadecane, Sodium dodecyl benzene sulfonate (SDBS) and ammonium persulfate were offered by Sinopharm chemical. Ferric sulfate nonahydrate($Fe(NO_3)_3 \cdot 9H_2O$) and Benzene-1,3,5-tricarboxylic acid (H_3BTC) were purchased from Sigma-Aldrich. All chemicals used in the experiment are analytical reagent without further purification.

2.2 Synthesis of MicroPCM

Compared with traditional desiccants, MOFs have greater moisture adsorption capacity and transfer rate due to their huge specific surface area and high porosity. However, the MOFs prepared in early literature had poor water stability, and the pore structure collapsed easily during the process of moisture desorption [26–29]. MOFs prepared by hydrothermal synthesis generally have better water stability. Here, we synthesis MIL-100(Fe) hydrothermally from metal Fe3+ ions and trimesic acid. MIL-100(Fe) shows great ability to adsorb moisture from air and can be obtained easily through large-scale synthesis [30–32], making it one of the best choices for humidity pump.

The water adsorption characteristics of MIL-100(Fe) were studied in previous research [21]. Fig. 1 shows the water adsorption isotherms of MIL-100(Fe) at various temperatures. It can be seen that the water adsorption isotherm of MIL-100(Fe) at 20 ◦C has a stepwise increase between 470 Pa (20% RH) and 1170 Pa (50% RH). This S-shaped isotherm can ensure that the cyclic water uptake is close to the maximum adsorption capacity of dry materials. The maximum difference in moisture content between 20 and 50 ◦C under 2100 Pa can reach 0.56 kg $kg^{-}1$, which means the MOF humidity pump possesses the greater potential of adsorption efficiency and has less sensible energy loss by regeneration, as compared to the ones using traditional desiccant such as silica gel.

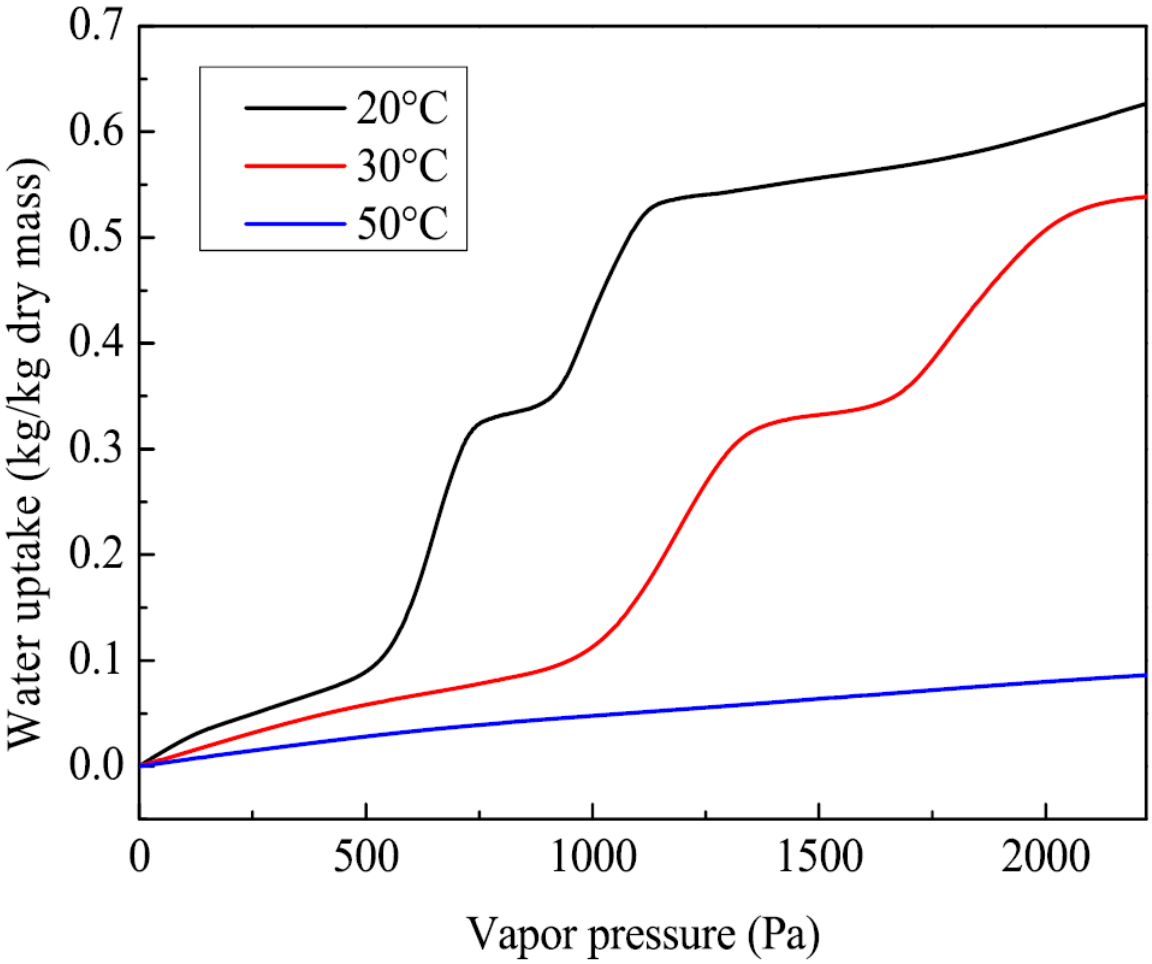

Fig. 1. Water adsorption isotherms of MIL-100(Fe) at different temperatures.

2.2 Humidity pump based on MIL-100(Fe)

A photograph of MOF based humidity pump is shown in Fig. 2(a). The humidity pump device is fabricated using two MOF coated heat exchangers (MOF-HEx) and two thermoelectric coolers, along with other components. Two aluminum-based plate fins type heat exchangers of the same size (100 mm(L) × 50 mm(W) × 60 mm(H)) are arranged symmetrically as the heat sinks. The plug-in HEx is comprised of 11 fins with a surface area of 0.132 m2 and 0.5 mm thickness each, while the width of the air channel between each fin is 4 mm. MIL-100(Fe) was coated on the surface of the fins by a water-borne binder of silica sol, which does not affect the water sorption characteristics and capacity.

The dry mass of the original heat exchangers and coated MIL-100(Fe) was characterized to be 199.6 g and 45.0 g, respectively. Two thermoelectric coolers (40 mm (L) × 40 mm (W) × 3.8 mm (H)) are stuck in the interlayer between the heat sinks by thermal grease to ensure sufficient contact. The rest of the part of heat sinks not covered by the thermoelectric coolers is blocked by silicon sealant to prevent heat transfer between the hot and cold ends.

Bonded heat sinks and thermoelectric coolers were integrated into an enclosed acrylic box (300 mm(L) × 60 mm(W) × 130 mm(H)) which was divided equally into two volumes by a partition plate. A rectangular cut-out is designed in the middle of the partition plate, corresponding to the size of the surface of the heat sink (100 mm × 50 mm). The periphery of the heat sinks and the partition plate is coated with hot melt adhesive to ensure that it is airtight. Both the upper and lower parts of the acrylic box have two vents of 50 mm diameter connected to the four-way valves and duct fan through the bellows.

A schematic diagram of the MOF based humidity pump is shown in Fig. 2(b). Thermoelectric coolers absorb and release heat at two opposite sides, according to the Peltier effect, when an electrical current passes through it. In this way, the adsorption heat during the dehumidification process is transferred to the other side to improve the temperature of the sink for regeneration. The exchange of dehumidification and regeneration can be achieved by reversal of electrical current and switching fourway valves.

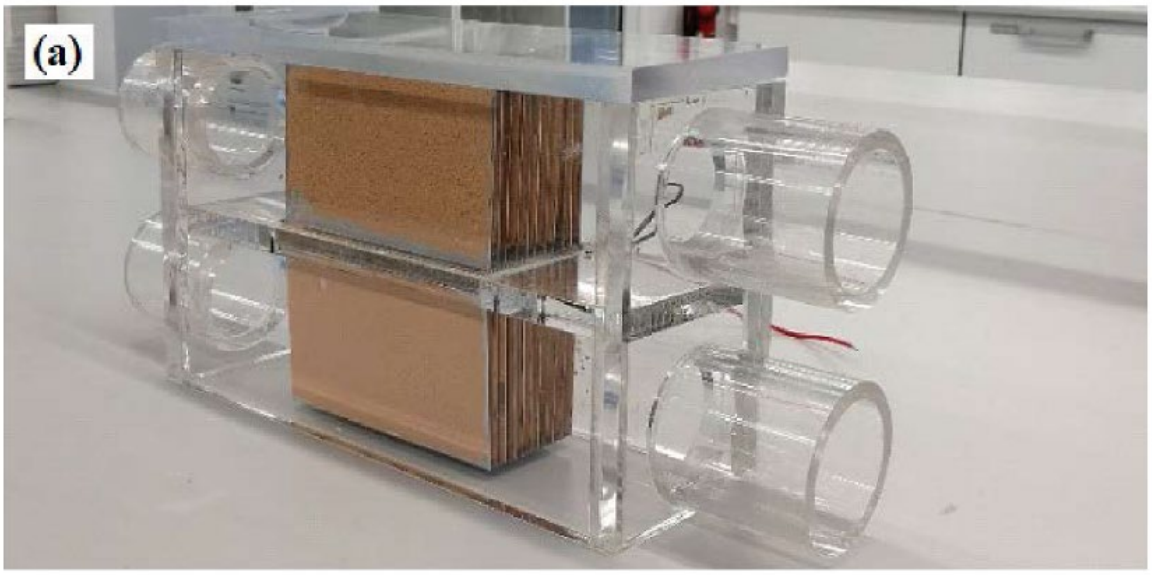

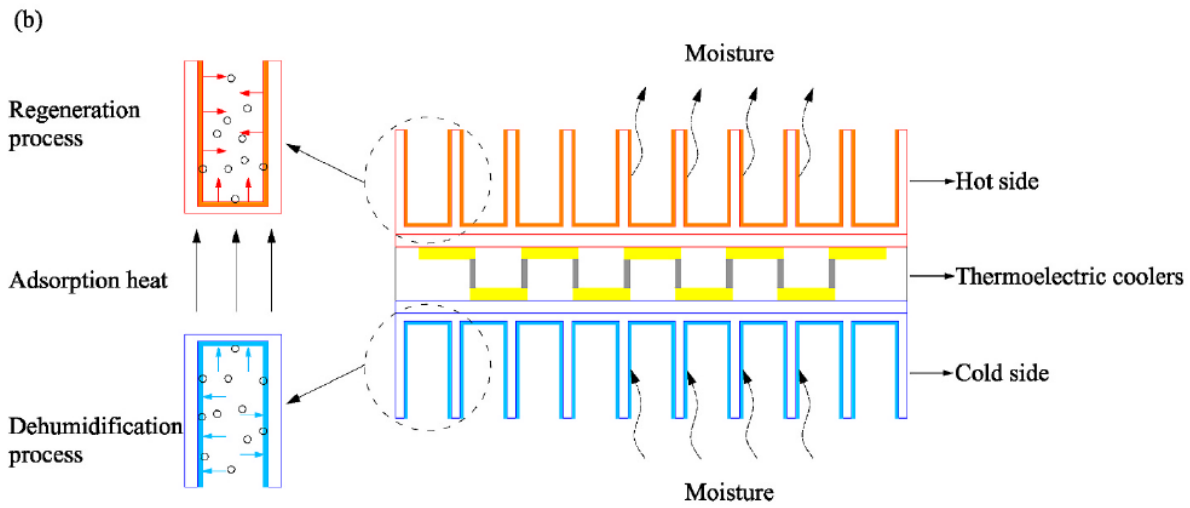

Fig. 2. Photograph and schematic diagram of MOF based humidity pump.

2.3 Working principle

The dehumidification and regeneration processes can be implemented simultaneously when the humidity pump starts running. The detailed working principles can be described in two parts as follows: Dehumidification: Typically, there are three ways to achieve dehumidification, namely isothermal dehumidification (O→B1), cooling and dehumidification (O→B2), and isenthalpic dehumidification (O→B3). The isothermal methods have been considered as most promising, reported in many refs [8,22], while the other two are, comparatively, not energy-efficient to some extent. In our humidity pump device, moisture can be adsorbed when humid air flows through the surface of MIL-100(Fe) coated fins on the cold side. The dehumidified air can thus be obtained with a subtle temperature rise (O–B shown in Fig. 3). Based on thermodynamic analysis, this can be explained by the total heat transferred on the dehumidification side, which consists of conduction and Joule heat from TEC module, convection heat from inlet air, adsorption heat from the desiccant, and the remaining heat during the switching. Theoretically, by regulating the input power and ventilation quantity, it is feasible to achieve a quick latent load control through a nearly isothermal dehumidification process, the way close to O→B1 (an ideal path).

Regeneration: As for an ideal regeneration condition, desorption of the trapped water vapor in an isothermal regeneration way (O→A1) is preferable. The main reason is that this can lower energy consumption massively. In actual conditions, it is difficult to achieve isothermal regeneration; it is, however, desirable to use fewer energy sources to bring more desorbed water vapor. Considering the interaction between water vapor molecules and desiccant, traditional materials such as zeolite require a high-temperature heat source (>90 ◦C) to go through

the regeneration process (O→A2), while MIL-100(Fe) can be regenerated easily with a relatively low-temperature heat source (~50 ◦C) [22]. In this regard, the heat and mass variation of regeneration air in our device should follow the O→A path, which is specifically between O→A2 and O→A1.

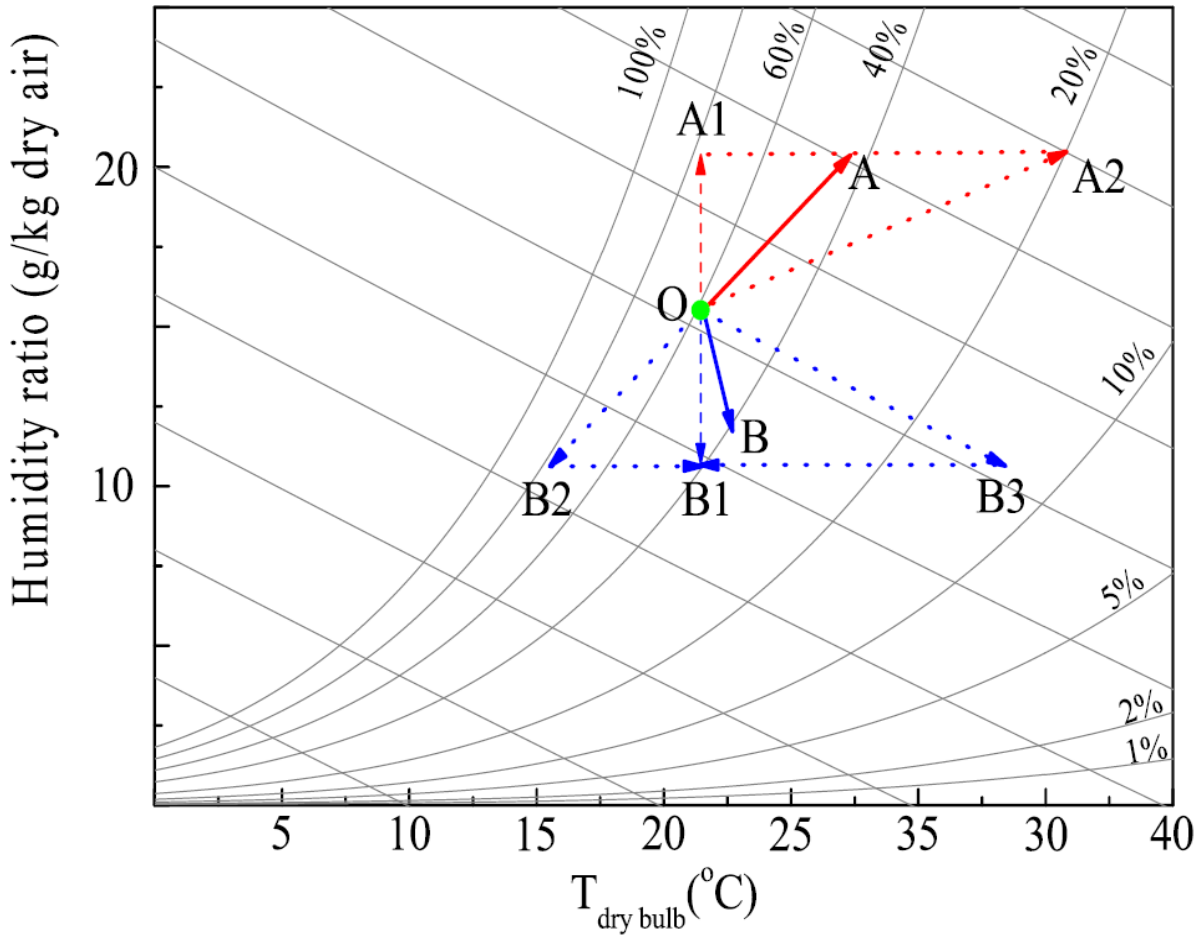

Fig. 3. Working principle: Psychrometric chart of the air treating process in our humidity pump.

2.4. Operation modes

In this paper, experiments have been carried out in two groups: 1) Mode A- Parameter studies. 2) Mode B- Operation performance of localized humidity control for a small test chamber. The operation parameters including inlet air conditions of dehumidification and regeneration sides are presented in Table 1.

Mode A (Test mode): In this mode, dynamic characteristic and parameter studies have been carried out. The humidity pump device is placed in the test room (like an air cleaner), and the inlet air of both the dehumidification and regeneration sides is the same indoor air. As shown in Fig. 4(a), when the indoor air flows through the dehumidification side, the moisture in the air is adsorbed on the desiccant coated on the fins, leading to a decrease in humidity level. The outlet air from the dehumidification side (dry air) is supplied indoors. Simultaneously, the other batch of indoor air enters the device through the inlet to the regeneration side, flows through the hot side and takes away the moisture released from the desiccant to dry the MOF coatings. The outlet of the regeneration side is exhausted to outdoor. When the desiccant in the dehumidification side saturates, the current flow direction of the thermoelectric cooler is reversed to interchange the roles of dehumidification and regeneration. Meanwhile, only one of the four-way valves (outlet) is rotated by 90◦ and the state is converted from A1 to A2. Such a reciprocating cycle can realize the continuous operation of the MOF humidity pump.

Mode B (Internal recycle mode): In this intended operation mode for real applications, the inlet air of dehumidification side is always the indoor air, while the inlet air of the regeneration side is always outdoor (ambient) air. The outlet air of the dehumidification side (dry air) is supplied to indoor again. The outlet air of the regeneration side (humid air) is exhausted outdoors. To

control the airflow direction, two fourway valves are used as shown in Fig. 4(b), and the airflow passages of the internal recycle channel and external channel are interchanged. The outdoor (ambient) air has no direct heat and mass transfer with the indoor air as these two airflows are completely separated. The outdoor airflow is only used to take away the heat and moisture released by MOF desiccants during the regeneration process. Through a reciprocating cycle, the MOF humidity pump can work continually under internal recycle mode.

2.5. Experimental measurement

Under working mode, the air was supplied to the humidity pump via a duct, and the power of the thermoelectric elements was adjusted andrecorded. There were no mechanical operations or moving parts in thewhole device. During the dehumidification and regeneration process, temperature and relative humidity of the inlet and outlet air were measured by using digital hygro sensors with accuracy of ±0.2 ◦C and ±2% RH (SEK-SHTC3-Sensors, Sensirion). The airflow rate was adjusted by variable frequency fan (LH-50P, Jiuyefeng Environmental Technology Co., Ltd.) and recorded by an anemograph (Testo 410-1). The current and voltage of the thermoelectric cooler and the fan under different conditions were recorded for the calculation of power consumed.

Table 1. Operation conditions of different modes.

Operation mode	Parameters	Values
Test mode	Inlet air conditions of De/Re side	22.8 °C, 60%RH
	Cycle time	5min, 10min, 15min
	Thermoelectric power	15 W, 20 W, 25 W
	Air velocity	1.5 m/s, 3.5 m/s, 4.2 m/ s
Internal recycle mode	Initial inlet air conditions	23 ◦C, 81%RH
	Cycle time	10min
	Thermoelectric power	30 W
	Air velocity	2.4 m/s

2.6 Performance indexes

To evaluate the performance of MOF-based humidity pump as a function of the power input and the temperature and humidity ratio of inlet and outlet air, some parameters herein have been analyzed: 1) Dehumidification rate (E_d): It represents the moisture removal over a period of time, which is computed as follows:

$$E_d = \frac{\int_{t_1}^{t_2} q_a(d_{in} - d_{out})dt}{\Delta t} \quad (1)$$

where E_d (g s^{-1}) is dehumidification rate; q_a (m3 s^{-1}) is the volume flow. d_{in} and d_{out} (g m^{-3}) are moisture content of inlet and outlet air during dehumidification process, respectively. t_1 and t_2 represent the beginning and end of a dehumidification process when it comes to equilibrium. Δ t is the time of one dehumidification process, and can be calculated by $\Delta t = t_2 - t_1$.

2) Moisture removal efficiency (η): It represents the power consumption (P_e) to approach to the dehumidification rate (E_d):

$$\eta = \frac{E_d}{P_e} \quad (2)$$

where η (g Wh-1) indicates the moisture removal efficiency. P_e (kW) is the total power consumption (including thermoelectric coolers and duct fans).

3) Dehumidification coefficient of performance (DCOP) represents the ratio of air enthalpy variation during the dehumidification process to the total power consumption for the regeneration process:

$$DCOP = \frac{q_a(h_{in} - h_{out})}{P_e} \quad (3)$$

where h_{in} and h_{out} are the air enthalpies of inlet and outlet process air.

3. Results and discussion

3.1 Dynamic characteristics

The dynamic characteristics of the device are analyzed in terms of temperature and humidity of inlet and outlet air. In order to compare the cycling performance of dehumidification and regeneration sides, inlet air conditions for these two sides were maintained the same. Thus, the detailed experimental conditions can be shown as follows: the temperature and relative humidity of inlet air are about 22.8 ◦C and 60%. The velocity of inlet air is 1.5 m/s. The current of the thermoelectric cooler is 2.66 A, its voltage is 11.32 V, and the calculated power is about 30 W.

When it comes to the equilibrium, Fig. 5 shows the variation of temperature and humidity at the inlet and outlet of dehumidification and regeneration sides. The operation consists of dehumidification and regeneration processes, and several cycles are performed until stabilization is reached. The period from 0 to 10 min is the regeneration process corresponding to the regeneration side. It can be seen that the temperature of the outlet air rises sharply at the beginning and then gradually flattens. The moisture content of the outlet air initially increased in line with the temperature, but then decreased gradually.

This is because the vapor in MIL-100 (Fe) coatings desorbs as the temperature of the heat exchanger rises sharply. As the desorption proceeds, water vapor content in the desiccant coating decreases gradually, along with the rate of desorption, resulting in a gradual decrease in the moisture content in the outlet air. The dehumidification and regeneration channels are switched over during the period from 10 to 20min. The outlet air temperature decreases rapidly;

but the temperature of the outlet air is, however, still higher than the inlet air. According to the thermodynamic analysis in the previous section, the cooling load of the cold side of TEC cannot remove all the sensible loads to be as cool as the inlet air, but the temperature rise was limited. The average outlet temperature at the dehumidification channel is close to 25.5 ◦C. Besides, the adsorption heat also increases the temperature of the air. At the same time, when the air flows through the heat exchanger, the water vapor in the air is adsorbed on the MIL-100 (Fe) coating, and the moisture content decreases sharply. As the coating material becomes saturated gradually from the outside to the inside of the layer, the dehumidification rate also decreases gradually.

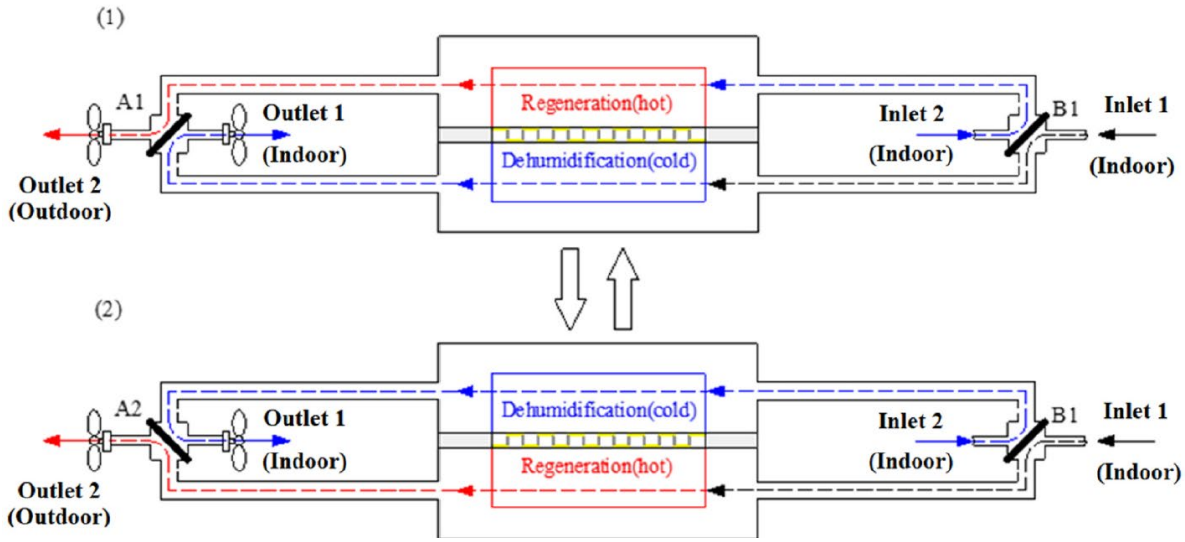

(a) Mode A: test mode

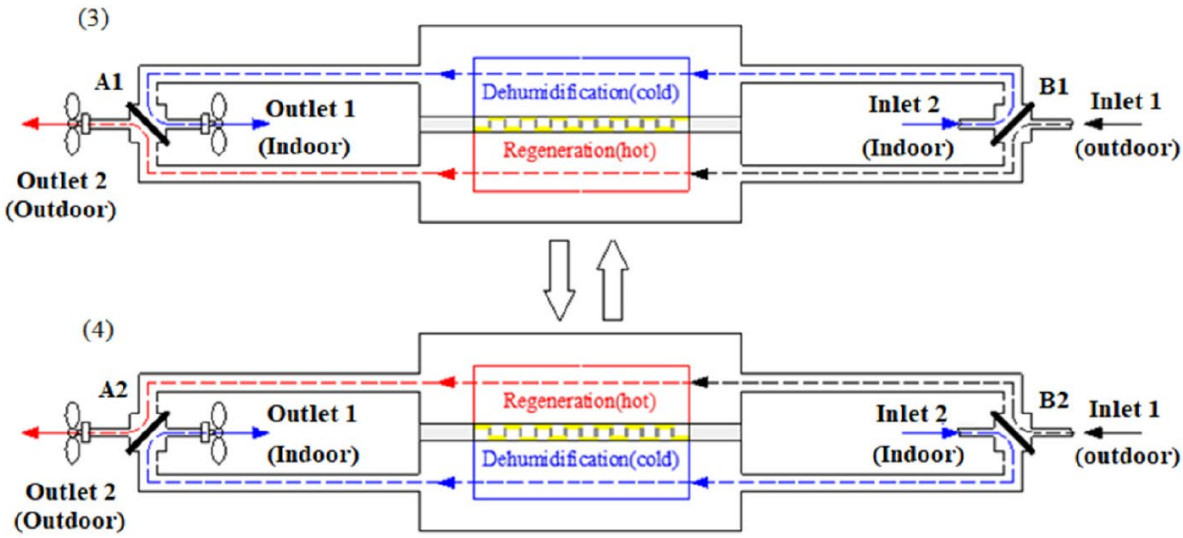

(b) Mode B: internal recycle mode

Fig 4. The operation modes of MOF humidity pump.

3.2 Performance of the humidity pump with different desiccants

Based on the same experimental conditions described in Section 3.1, inlet air condition remains at 22.8 ◦C and 60%RH. Air velocity is set at 1.5 m/s. The power of thermoelectric cooler is around 30 W. From Fig. 6, it shows the difference in moisture content between the inlet and outlet air of the humidity pump with silica gel and MIL-100(Fe) coatings. It can be seen that the humidity pump with MIL-100(Fe) coating shows greater adsorption and desorption rate than that of the silica gel coating while the attenuation rate is slower. This happens because the regeneration temperature of MIL-100 (Fe) is lower, and the moisture storage capacity is larger than that of silica gel. The operation indices are calculated based on Eqs. (1) and (2). The dehumidification rate and moisture removal efficiency of humidity pump with silica gel coating are 12.23 g h^{-1} and 0.41 g Wh^{-1}, respectively, and for MIL-100(Fe) coating are 26.24 g $^{h-1}$ and 0.87 g Wh^{-1}, respectively. The values of the MOF based humidity pump were 2.15 and 2.12

times greater than that of silica gel.

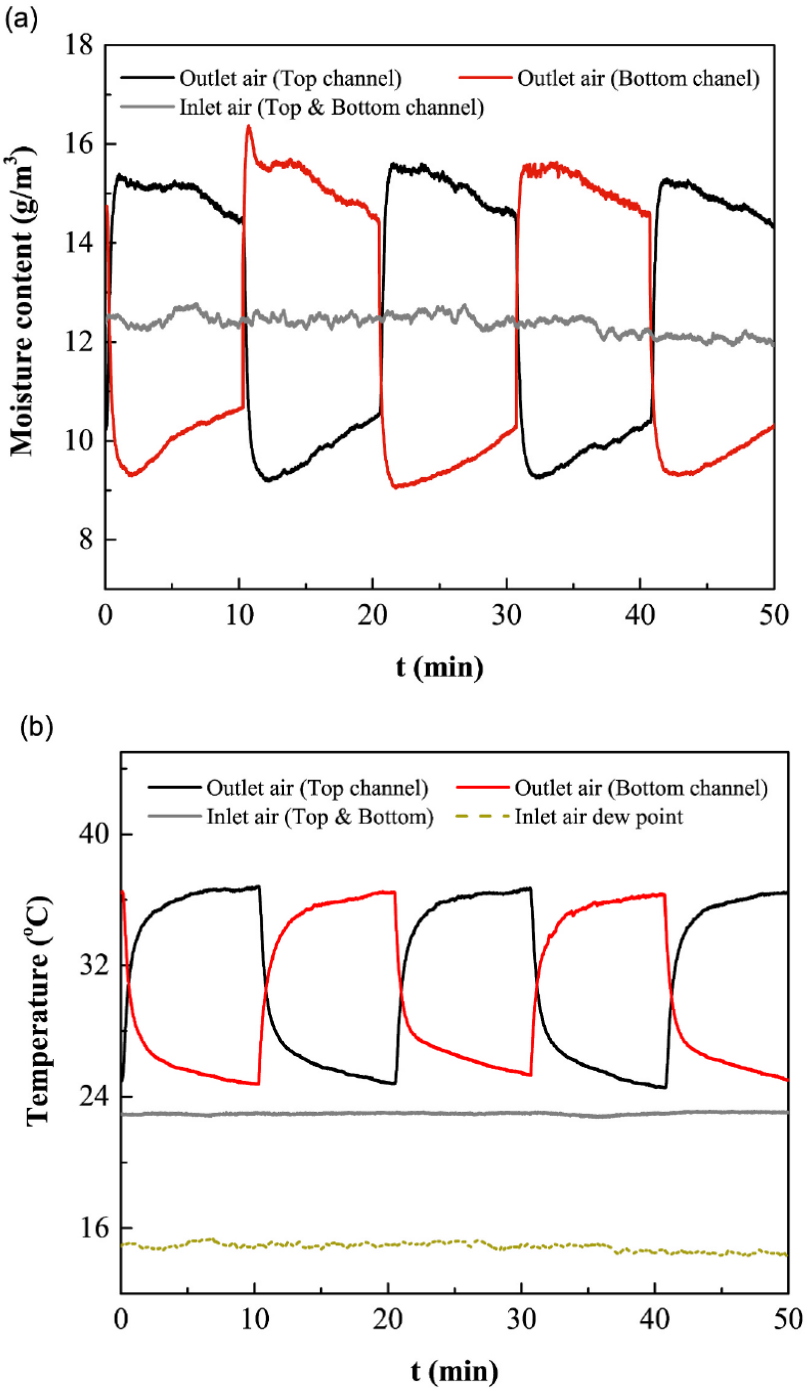

Fig. 5. Temperature and moisture content of inlet and outlet air in Mode A.

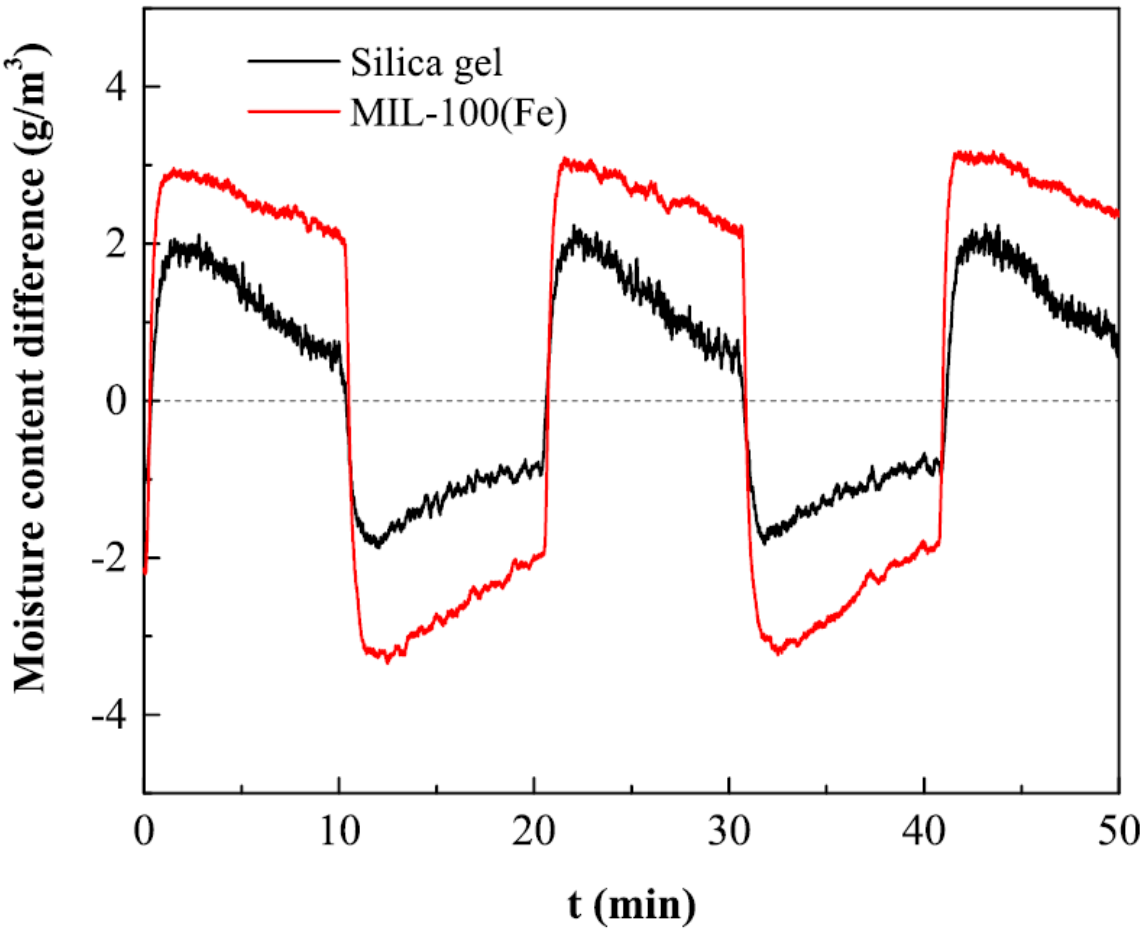

Fig. 6. Moisture content difference of humidity pump using silica gel and MIL-100(Fe).

3.3. Dehumidification performance

3.3.1. Cycle time

According to the previous analysis of dynamic characteristics, it can be observed that as the operating time goes on, the moisture removed by MIL-100(Fe) coating decreases gradually. This indicates that the cycle time has an important effect on the performance of the device. The thermoelectric power is maintained at 30 W while the air speed is 1.5 m/s. A series of experiments with different cycle times were carried out. The moisture content difference between the inlet and outlet air of the humidity pump is shown in Fig. 7. As the cycle time increases from 5 to 10 and 15min, the peak value of moisture content difference decreases from

-3.10 to -3.35 and -3.38 g $^{m-3}$ at the dehumidification side, and increases from 2.92 to 3.18 and 3.39 g m^{-3} at the regeneration side, respectively. The absolute values of maximum moisture content difference increase with the increase in cycle time because the regeneration of desiccant becomes sufficient as the cycle time increases. It can also be seen from Fig. 7 that the attenuation of moisture content difference is more serious with the increase in cycle time as the desiccant coating saturates gradually, with the increase of operating cycle time, and the dehumidification capacity decreases.

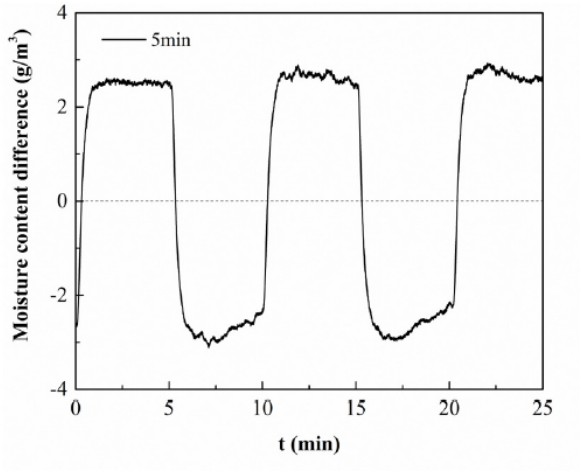

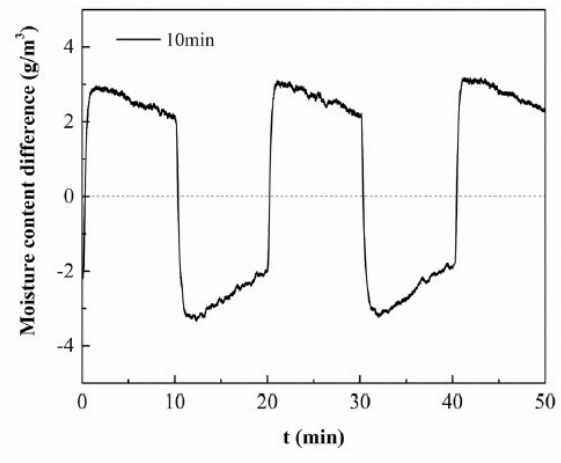

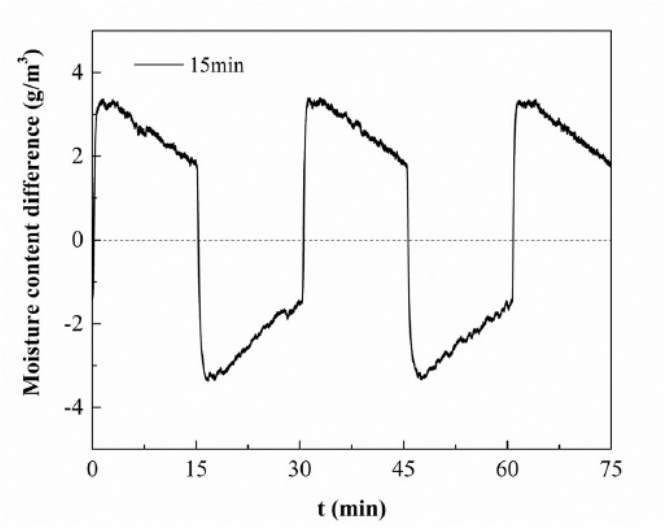

Fig. 7. Moisture content difference of humidity pump with the different cycle times.

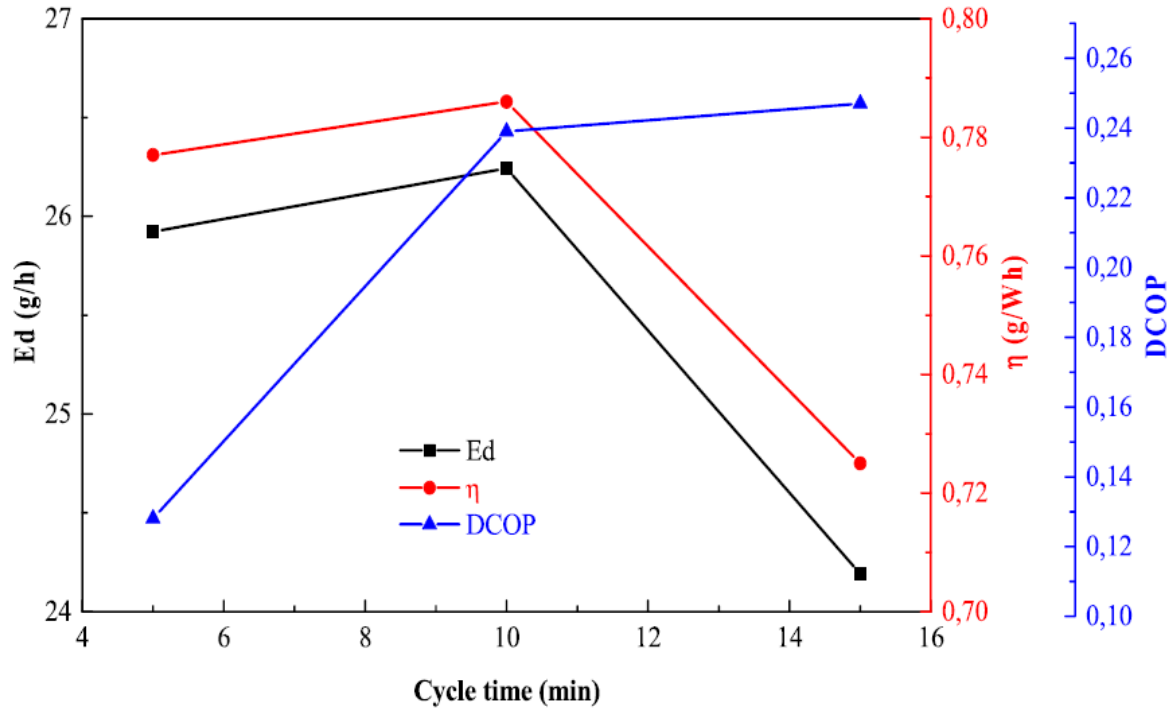

Fig. 8. Effect of cycle time on the performance of humidity pump.

Fig. 8 shows the effect of cycle time on the performance of the humidity pump. It can be seen that the dehumidification rate and moisture removal efficiency increase at first and then decrease with the increase in cycle time, determined by the peak value of the moisture content difference and the decay degree. This can be attributed to the decay characteristics of the adsorption and regeneration ability of the MIL-100 (Fe) layers at different cycle times.

DCOP increases as the cycle time increases, but the rate of the rise is restricted after 10min of cycle time in our case.

3.3.2. Thermoelectric power

Thermoelectric power, which has an important effect on the regeneration of the desiccant layer, determined the temperature difference between the hot and cold sides. The cycle time is set to 10 min and the air speed is 1.5 m/s. Several experiments with different input power of the thermoelectric cooler are carried out and the moisture content differences between the inlet and outlet air of the humidity pump are shown in Fig. 9. Comparing the moisture content difference between the three cases, it can be seen that the lower the power, the smaller the moisture content difference between the inlet and outlet air. Particularly at 15 W, there is almost no dehumidification ability at the end of the cycle time. Further analysis found that as the mode changed from dehumidification to regeneration, the moisture content difference first rises rapidly and then drops sharply, a tip is formed. Thus, the lower the thermoelectric power, the sharper the tip is. Insufficient power results in lower temperature differences between the hot and cold sides affecting the regeneration of the desiccant layer.

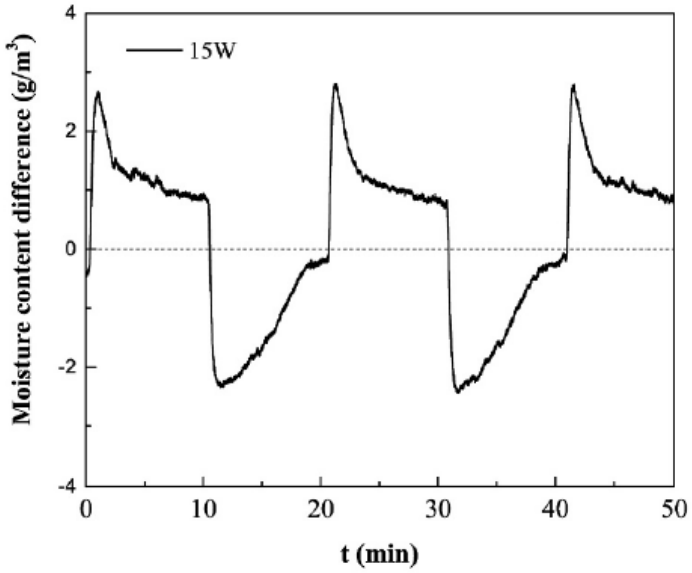
15W
Moisture content difference (g/m3)
t (min)
4
2
0
-2
-4
0
10
20
30
40
50

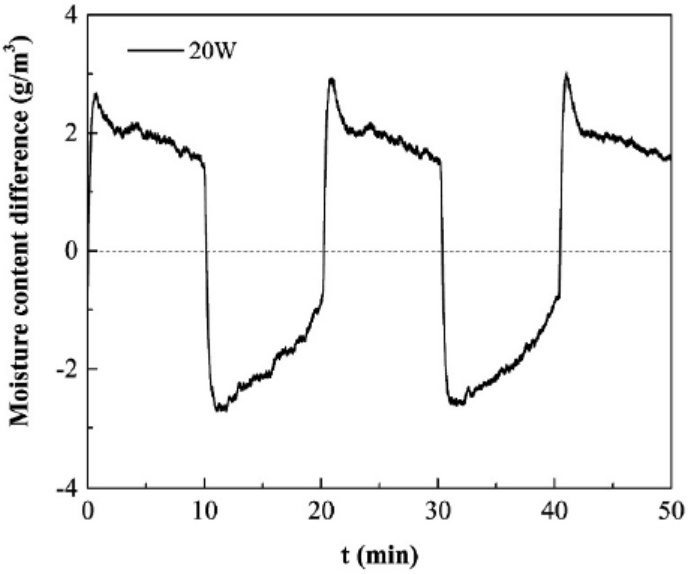
20W
Moisture content difference (g/m3)
t (min)
4
2
0
-2
-4
0
10
20
30
40
50

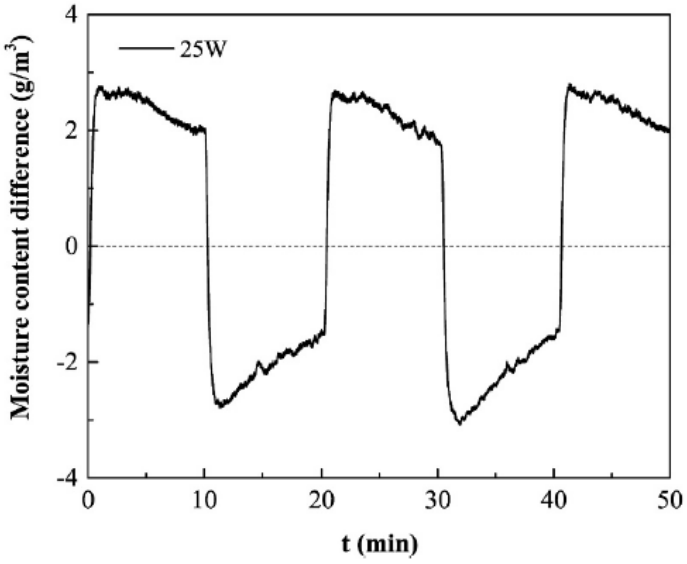

Fig. 9. Moisture content difference of humidity pump with different power.

Fig. 10 shows the impact of thermoelectric power on the performance of the humidity pump. With the increase of thermoelectric power from 15 W to 25 W, the dehumidification rate increases from 20.5 to 31.9 g h□ 1, suggesting that the dehumidification rate increases with the increase of thermoelectric power. The greater the thermoelectric power, the higher the temperature of the hot side, and the better the regeneration. The moisture removal efficiency increases at first and then decreases with the increase of thermoelectric power showing the same changing trend as DCOP. In this regard, too high thermoelectric power would have a negative impact on moisture removal efficiency and DCOP. As the thermoelectric power increases to a certain degree, the temperature achieved is enough for the regeneration of MIL-100 (Fe). Excessive power will increase the energy consumption and will have no obvious effect on improving regeneration efficiency.

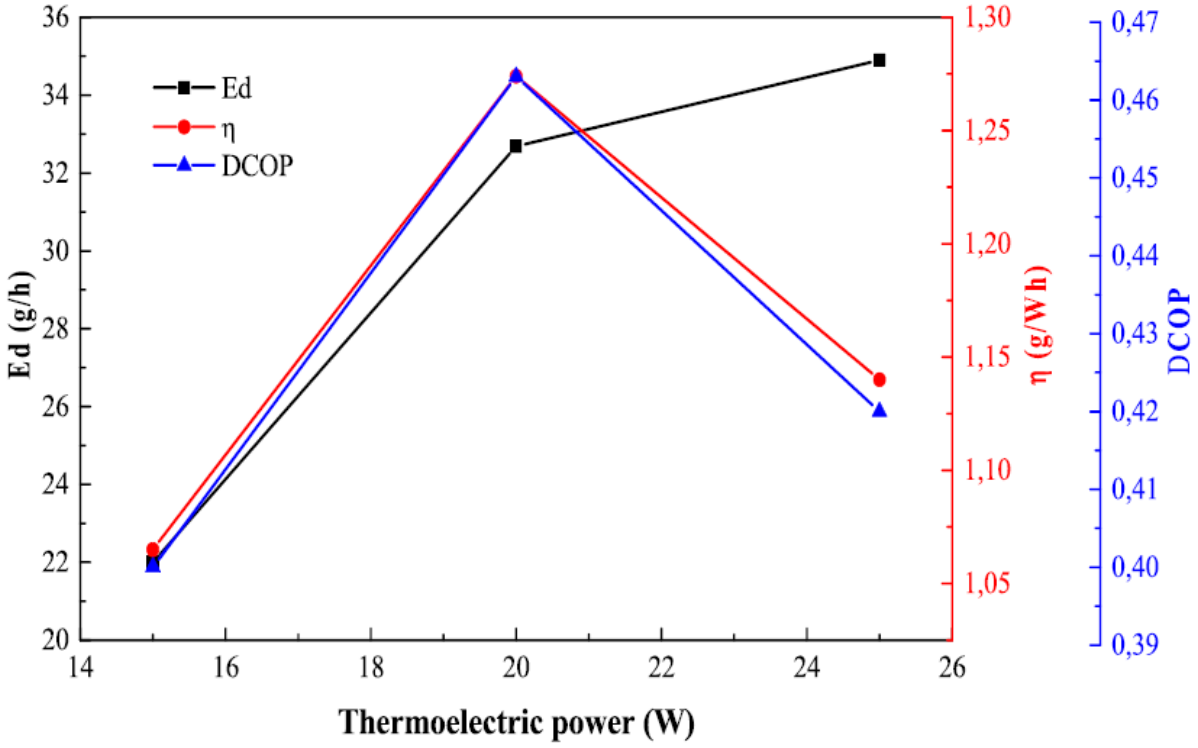

Fig. 10. Effect of thermoelectric power on the performance of humidity pump.

3.3.3. Air velocity

Air velocity is another important factor of the humidity pump. The cycle time is set to 10 min and the thermoelectric power was 30 W. Several experiments with variable air velocity are carried out, and the moisture content difference between inlet and outlet air of the humidity pump is shown in Fig. 11. As the air velocity increases, the peak value of moisture content difference between the inlet and outlet air during dehumidification and regeneration processes decreases. On the one hand, airflow increases with the increasing air velocity, which would increase the moisture content of the air, while on the other hand, heat transfer of the fins is enhanced by increasing the air velocity. This would reduce the temperature of the heat sink and the regeneration performance.

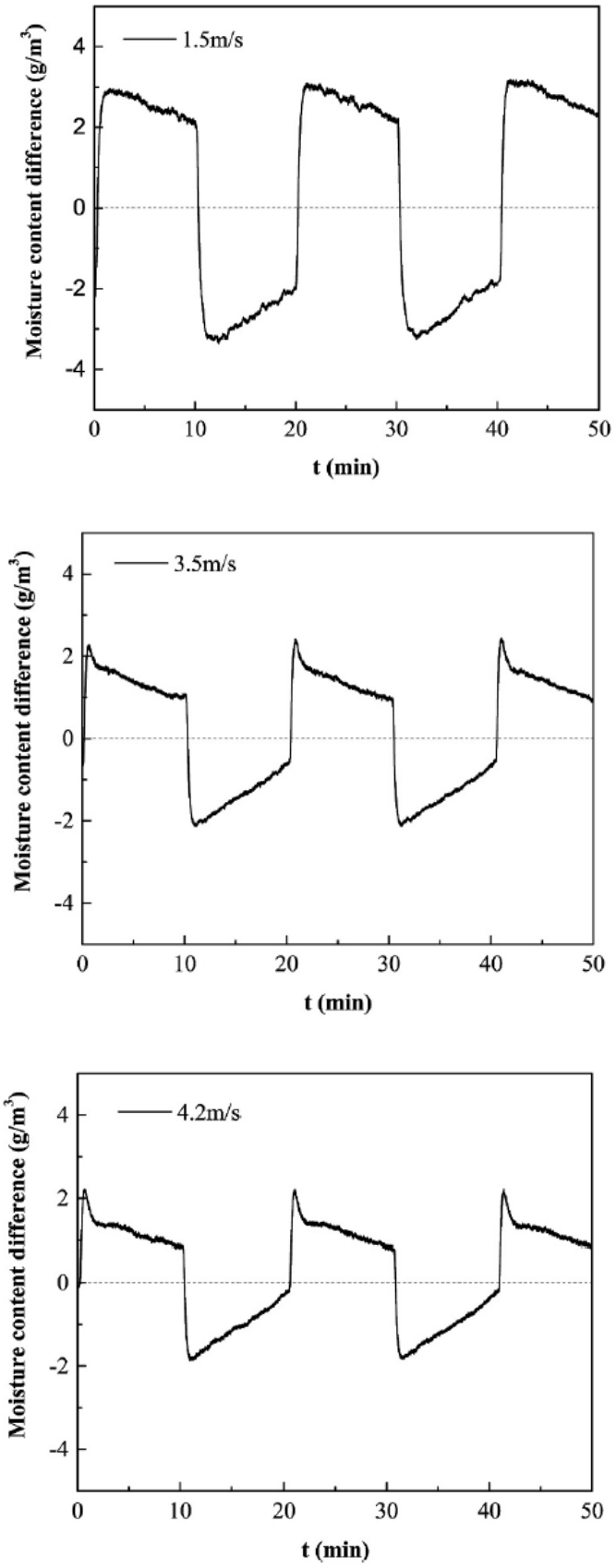

Fig. 11. Moisture content difference of humidity pump with different air velocity.

Fig. 12 shows the effect of air velocity on the performance of the humidity pump. Both the dehumidification rate and moisture removal efficiency increase first and then decrease as the air velocity increases. Also, excessive air velocity has a negative effect on the performance of the humidity pump owing to the reduction in regeneration temperature on the hot sides with the increase in air velocity. Besides, the energy consumption of the pump also increases with increasing air velocity. However, based on our measured results, it can be found that DCOP can be raised linearly with the air velocity. Based on comprehensive consideration (E_d, η and DCOP), there is an equilibrium point for air velocity around 3.5 m/s.

3.4. Humidity control ability

In order to investigate the actual humidity management ability when exposed to a real conditions, a test chamber (32.5 × 54 × 40.3 cm) made of polystyrene foam (insulation material) is prepared for the humidity pump dehumidification experiment. The initial conditions are maintained at 23 ℃ and 81% RH (average value), while there are no heat or moisture dissipation sources in the experimental system. The box is connected to the humidity pump by plastic bellows. The schematic diagram of the experimental system is shown in Fig. 13, and the operating conditions are shown as follows: the cycle time is set to 10 min, the thermoelectric power is 30 W, and the air velocity is 2.4 m/s. The digital hygro sensors are installed to record the temperature and humidity variation against time.

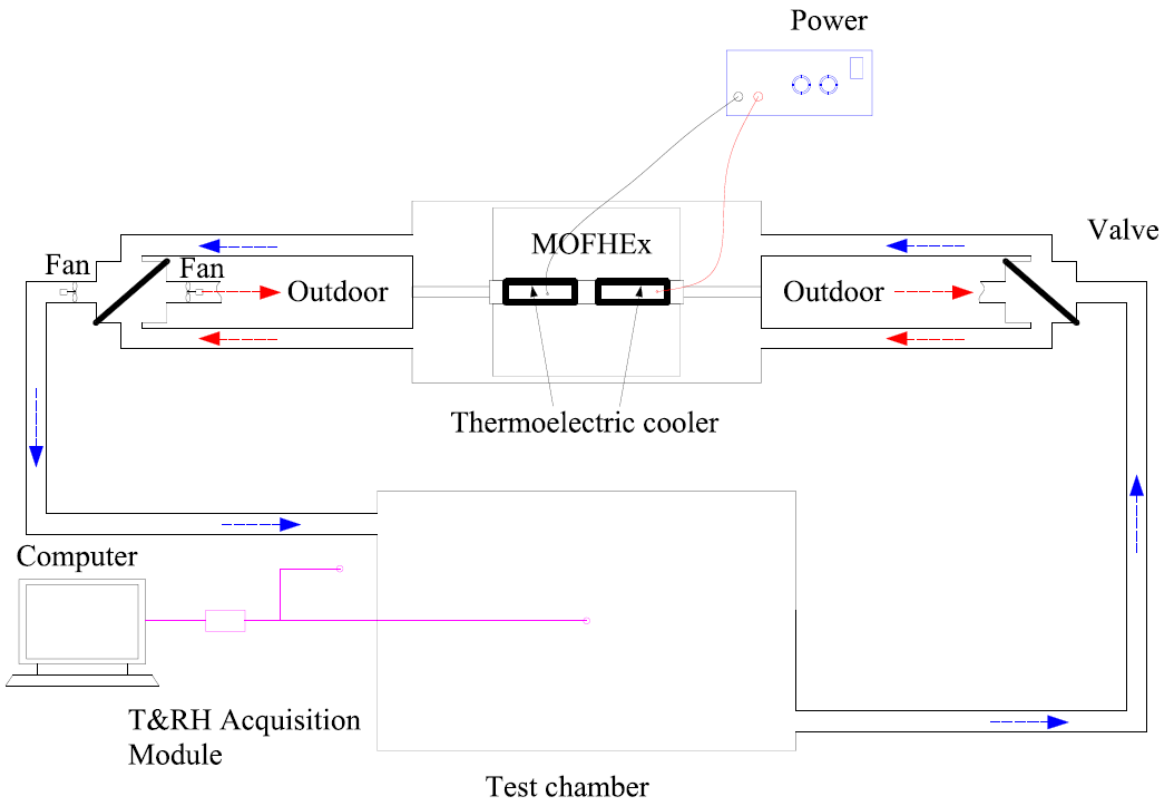

Fig. 13. Schematic diagram of the experimental system.

Fig. 14 shows the temperature and humidity conditions inside the test chamber during the experiments. Here, the measured results indicate that the temperature in the interior space fluctuates in a zigzag manner. Compared with the environment, the maximum temperature rise in interior space during the experiment is 1.52 ◦C over 1.3 h, as the fin temperature cannot be reduced immediately when the regeneration process is switched to the dehumidification process. The relative humidity of the interior space is decreased quickly from ~80% to 38%RH, corresponding to the absolute humidity from 16.7 to 8.2 g m^{-3}. There are no heat source and moisture dissipation sources inside the test chamber, as mentioned above. It is important to mention that the interior relative humidity stops decreasing at the trigger point of MOF desiccants, which is around 40% for MIL-100(Fe). It means that MIL-100 (Fe) stops adsorbing a large amount of moisture when the indoor RH is below 40%, and can be seen clearly from

the water sorption isotherm of MIL-100(Fe) [33]. It is known that many MOFs have S-shape isotherms and exhibit a steep uptake isotherm at the specific relative humidity depending on the targeted application [34]. For indoor humidity control, the steep uptake should around 40%. This can be noted as one of the main advantages of MOFs over other conventional desiccants. Some MOF materials can control indoor relative humidity autonomously, within the desired comfort range at room temperature [35]. Additionally, different MOFs have different trigger points and can be used for different moisture control applications [34,35]. Based on our measurements, it is seen that MIL-100(Fe) based humidity pump has a satisfactory response to handle the latent load of the test chamber.

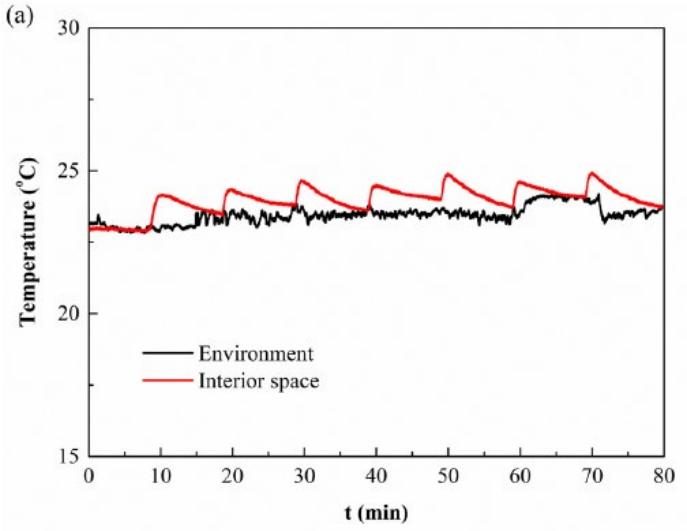

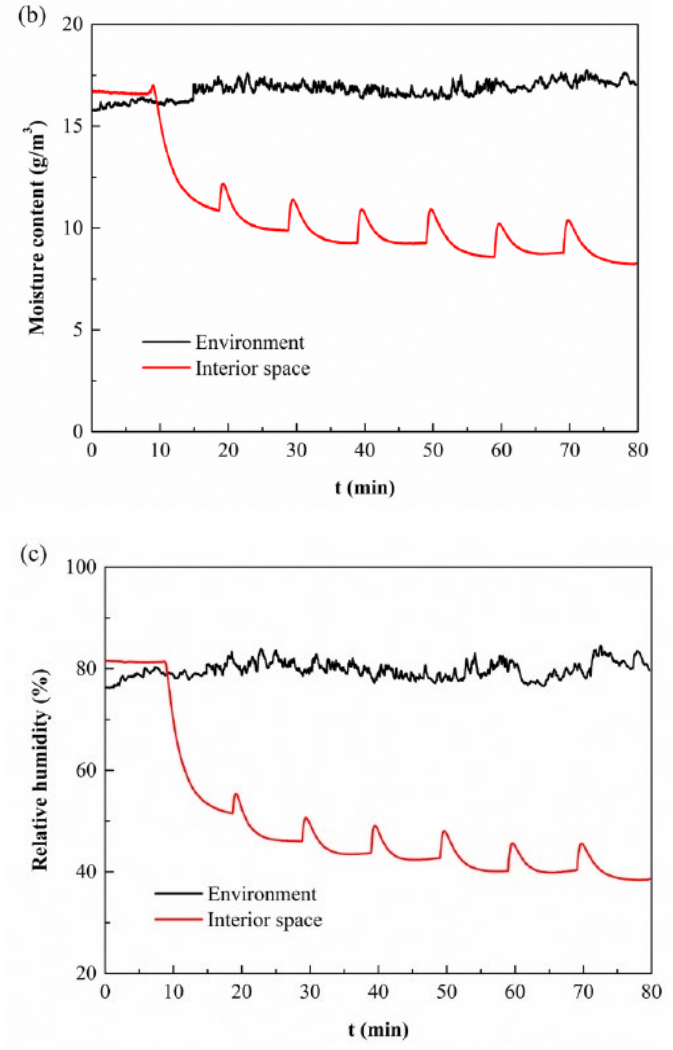

Fig. 14. Temperature and humidity changes inside the test chamber.

4. Conclusion

In this paper, a novel humidity pump that uses MOF as desiccant layers has been demonstrated. A series of experiments were carried out to investigate the dynamic characteristics and factors including cycle time, thermoelectric power, and air velocity. The dehumidification rate, moisture removal efficiency and DCOP were also calculated under different conditions. The conclusions are summarized as follows: (1) The humidity pump can be used to achieve dehumidification above the dew point temperature, thereby improving the dehumidification efficiency. Latent heat and adsorption heat can be handled by the desiccant layer and

thermoelectric cooler, respectively, which can realize the dehumidification and regeneration processes simultaneously. Four-way valves are used to achieve the continuous operation of the humidity pump and the conversion of the operation mode, making the mechanical system simplified. (2) The dehumidification performance of the humidity pump that uses MIL-100(Fe) as the desiccant layer is superior to that of the humidity pump that uses silica gel. The dehumidification rate, moisture removal efficiency, and DCOP of the MOF based humidity pump are found to be as high as 34.9 g h^{-1}, 1.14 g Wh^{-1}, and 0.46, respectively, which are all around twice higher than that of silica gel coated systems. (3) The dehumidification rate and moisture removal efficiency increase at first and then decrease with the increase of cycle time and air velocity, while the DCOP increases as the temperature rises. The dehumidification rate also increases with the increase of thermoelectric power. The moisture removal efficiency and DCOP increase first and then decrease with the increase of thermoelectric power. A too high thermoelectric power may have a negative impact on the moisture removal efficiency and DCOP. (4) The MOF based humidity pump achieves a quick localized humidity control. The internal relative humidity level can thus be maintained at the trigger point of MOF desiccants.

Acknowledgements

P. Hou and K. Zu would like to thank the China Scholarship Council for financial support to stay at the Technical University of Denmark (NO. 201803170122 and No. 201806230288). The authors acknowledge the financial support from Bjarne Saxhof's Foundation and the support from the Department of Civil Engineering at the Technical University of Denmark.

Conflicts of interest

The authors declare that they have no known competing financial interests or personal relationships that could have appeared to influence the work reported in this paper. All authors declare no conflict of interest.

References

[1] IEA, Energy Technology Perspectives, International Energy Agency, 2017, 2017. ISBN978-92-64-27597-3.

[2] Z. Wu, M. Qin, M. Zhang, Phase change humidity control material and its impact on building energy consumption, Energy Build. 174 (2018) 254–261.

[3] M. Qin, J. Yang, Evaluation of different thermal models in EnergyPlus for calculating moisture effects on building energy consumption in different climate conditions, Build. Simulat. 9 (2016) 15–25.

[4] F. Zhang, Y. Yin, X. Zhang, Performance analysis of a novel liquid desiccant evaporative cooling fresh air conditioning system with solution recirculation, Build. Environ. 117 (2017) 218–229.

[5] K. Chua, S. Chou, W. Yang, J. Yan, Achieving better energy-efficient air conditioning–a review of technologies and strategies, Appl. Energy 104 (2013) 87–104.

[6] R. Yumrutas¸, M. Kunduz, M. Kano˘glu, Exergy analysis of vapor compression refrigeration systems, Exergy Int. J. 2 (2002) 266–272.

[7] A. Chan, V. Yeung, Implementing building energy codes in Hong Kong: energy savings, environmental impacts and cost, Energy Build. 37 (2005) 631–642.

[8] B. Li, L. Hua, Y. Tu, R. Wang, A full-solid-state humidity pump for localized humidity control, Joule 3 (6) (2019) 1427–1436.

[9] M. Sultan, I. El-Sharkawy, T. Miyazaki, B. Saha, S. Koyama, An overview of solid desiccant dehumidification and air conditioning systems, Renew. Sustain. Energy Rev. 46 (2015) 16–29.

[10] K. Rambhad, P. Walke, D. Tidke, Solid desiccant dehumidification and regeneration methods-A review, Renew. Sustain. Energy Rev. 59 (2016) 73–83.

[11] L. Mei, Y. Dai, A technical review on use of liquid-desiccant dehumidification for air-conditioning application, Renew. Sustain. Energy Rev. 12 (2008) 662–689.

[12] A. Lowenstein, Review of liquid desiccant technology for HVAC applications, HVAC R Res. 14 (2008) 819–839.

[13] C. Isetti, E. Nannei, A. Magrini, On the application of a membrane air—liquid contactor for air dehumidification, Energy Build. 25 (1997) 185–193.

[14] B. Yang, W. Yuan, F. Gao, B. Guo, A review of membrane-based air dehumidification, Indoor Built Environ. 24 (2015) 11–26.

[15] A. Yadav, V. Bajpai, Experimental comparison of various solid desiccants for regeneration by evacuated solar air collector and air dehumidification, Dry. Technol. 30 (2012) 516–525.

[16] K. Gommed, G. Grossman, Experimental investigation of a liquid desiccant system for solar cooling and dehumidification, Sol. Energy 81 (2007) 131–138.

[17] L. Zhang, N. Zhang, A heat pump driven and hollow fiber membrane-based liquid desiccant air dehumidification system: modeling and experimental validation, Energy 65 (2014) 441–451.

[18] T. Ge, Y. Dai, R. Wang, Z. Peng, Experimental comparison and analysis on silica gel and polymer coated fin-tube heat exchangers, Energy 35 (2010) 2893–2900.

[19] X. Sun, Y. Dai, T. Ge, Y. Zhao, R. Wang, Comparison of performance characteristics of

desiccant coated air-water heat exchanger with conventional air-water heat exchanger–Experimental and analytical investigation, Energy 137 (2017) 399–411.
[20] S. Chai, X. Sun, Y. Zhao, Y. Dai, Experimental investigation on a fresh air dehumidification system using heat pump with desiccant coated heat exchanger, Energy 171 (2019) 306–314.
[21] S. Andres, X. Sun, T. Ge, Y. Dai, R. Wang, Experimental investigation on performance of a novel composite desiccant coated heat exchanger in summer and winter seasons, Energy 166 (2019) 506–518.
[22] S. Cui, M. Qin, A. Marandi, V. Steggles, S. Wang, et al., Metal-Organic Frameworks as advanced moisture sorbents for energy-efficient high temperature cooling, Sci. Rep. 8 (2018) 15284.
[23] X. Zheng, T. Ge, R. Wang, Recent progress on desiccant materials for solid desiccant cooling systems, Energy 74 (2014) 280–294.
[24] G. F´erey, C. Mellot-Draznieks, C. Serre, F. Millange, J. Dutour, et al., A chromium terephthalate-based solid with unusually large pore volumes and surface area, Science 309 (2005) 2040–2042.
[25] O. Yaghi, M. O'Keeffe, N. Ockwig, H. Chae, M. Eddaoudi, et al., Reticular synthesis and the design of new materials, Nature 423 (2003) 705.
[26] A. Cadiau, Y. Belmabkhout, K. Adil, P. Bhatt, R. Pillai, et al., Hydrolytically stable fluorinated metal-organic frameworks for energy-efficient dehydration, Science 356 (2017) 731–735.
[27] D. Alezi, I. Spanopoulos, C. Tsangarakis, A. Shkurenko, K. Adil, et al., Reticular chemistry at its best: directed assembly of hexagonal building units into the awaited metal-organic framework with the intricate polybenzene topology, pbz- MOF [J], J. Am. Chem. Soc. 138 (2016) 12767–12770.
[28] P. Bhatt, Y. Belmabkhout, A. Cadiau, K. Adil, O. Shekhah, et al., A fine-tuned fluorinated MOF addresses the needs for trace CO2 removal and air capture using physisorption, J. Am. Chem. Soc. 138 (2016) 9301–9307.
[29] J. Low, A. Benin, P. Jakubczak, J. Abrahamian, S. Faheem, et al., Virtual high throughput screening confirmed experimentally: porous coordination polymer hydration, J. Am. Chem. Soc. 131 (2009) 15834–15842.
[30] P. Horcajada, S. Surbl´e, C. Serre, D. Hong, Y. Seo, et al., Synthesis and catalytic properties of MIL-100 (Fe), an iron (III) carboxylate with large pores, Chem. Commun. (J. Chem. Soc. Sect. D) (2007) 2820–2822.
[31] Y. Seo, J. Yoon, J. Lee, U. Lee, Y. Hwang, et al., Large scale fluorine-free synthesis of hierarchically porous iron (III) trimesate MIL-100 (Fe) with a zeolite MTN topology, Microporous Mesoporous Mater. 157 (2012) 137–145.
[32] P. Hou, M. Qin, S. Cui, K. Zu, Preparation and characterization of metal-organic framework/microencapsulated phase change material composites for indoor hygrothermal control, J. Build. Eng. 31 (2020) 101345.
[33] X. Feng, M. Qin, S. Cui, C. Rode, Metal-organic framework MIL-100(Fe) as a novel moisture buffer material for energy-efficient indoor humidity control, Build. Environ. 145 (2018) 234–242.
[34] K. Zu, M. Qin, S. Cui, Progress and potential of metal-organic frameworks (MOFs) as

novel desiccants for built environment control: a review, Renew. Sustain. Energy Rev. 133 (2020), 110246.
[35] M. Qin, P. Hou, Z. Wu, J. Huang, Precise humidity control materials for autonomous regulation of indoor moisture, Build. Environ. 169 (2020), 106581.